

# ChemComm

Accepted Manuscript



This is an *Accepted Manuscript*, which has been through the Royal Society of Chemistry peer review process and has been accepted for publication.

*Accepted Manuscripts* are published online shortly after acceptance, before technical editing, formatting and proof reading. Using this free service, authors can make their results available to the community, in citable form, before we publish the edited article. We will replace this *Accepted Manuscript* with the edited and formatted *Advance Article* as soon as it is available.

You can find more information about *Accepted Manuscripts* in the [Information for Authors](#).

Please note that technical editing may introduce minor changes to the text and/or graphics, which may alter content. The journal's standard [Terms & Conditions](#) and the [Ethical guidelines](#) still apply. In no event shall the Royal Society of Chemistry be held responsible for any errors or omissions in this *Accepted Manuscript* or any consequences arising from the use of any information it contains.

Cite this: DOI: 10.1039/c0xx00000x

www.rsc.org/xxxxxx

ARTICLE TYPE

# Reversible catalysis for the reaction between methyl orange and NaBH<sub>4</sub> by silver nanoparticles

Li-Qing Zheng, Xiao-Dong Yu,\* Jing-Juan Xu and Hong-Yuan Chen

Received (in XXX, XXX) Xth XXXXXXXXXX 20XX, Accepted Xth XXXXXXXXXX 20XX

DOI: 10.1039/b000000x

The reaction between MO and NaBH<sub>4</sub> catalyzed by Ag NPs has been studied. Ag NPs catalyzed the reduction of MO rapidly, while adding CTAB into the solution caused the regeneration of MO. Thus, the reversible catalysis for the reaction between MO and NaBH<sub>4</sub> by Ag NPs was first discovered.

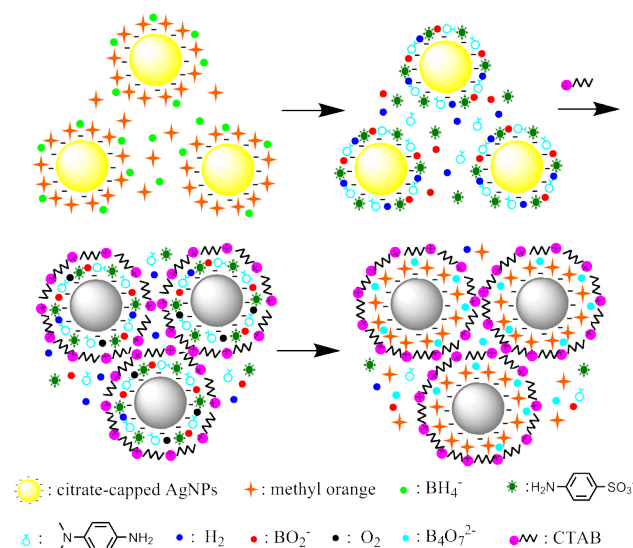
Recent years, nanoparticles of noble metal, such as Au, Ag, Pd and Pt, have played vital roles in chemistry research area because of their inherently robust physical and chemical properties.<sup>1</sup> With the special distance and size dependent surface plasmon resonance (SPR) property<sup>2</sup> and catalytic ability<sup>3</sup>, nanoparticles had potential applications as promising candidate of sensors and catalysts. For example, gold nanoparticles (Au NPs) and silver nanoparticles (Ag NPs) have been widely used in sensing<sup>4</sup> and catalysis<sup>5</sup>. The SPR properties and catalytic abilities of Au NPs and Ag NPs could be regulated by functionalizing and aggregating the nanoparticles.

It is observed that the optical properties of Au NPs and Ag NPs are tunable throughout the visible and near-IR regions of the spectrum as a function of the size, shape and local environment of nanoparticles.<sup>6</sup> For example, the color of dispersed Ag NPs solution is yellow while the highly aggregated Ag NPs solution turns out to be red.<sup>7</sup> There are various mechanisms of the aggregation of metal nanoparticles have been reported, such as electrostatic interaction<sup>8</sup>, complexation with ligand<sup>9</sup>, antibody-antigen associations<sup>10</sup>, streptavidin-biotin binding<sup>11</sup>, etc. Recently, our group has reported that the aggregation of Ag NPs could be induced by hydrophobic effect.<sup>12</sup>

Differently modified Au NPs and Ag NPs can catalyze various types of reactions including the reduction reaction, the oxidation reaction and polymerization reaction. For example, the modified Au NPs and Ag NPs can catalyze the reduction of methyl orange (MO)<sup>6,13</sup>, methyl blue (MB)<sup>14</sup> and 4-nitrophenol (4-NP)<sup>15</sup>, the oxidation of 2,2'-azino-bis (3-ethylbenzothiazoline-6-sulfonic acid) diammonium salt (ABTS) and 3,3,5,5-tetramethylbenzidine (TMB)<sup>16</sup>, and the polymerization of alkylsilanes<sup>17</sup>, etc. Au NPs and Ag NPs catalysts showed distinct advantages because their synthesis and functionalization are very simple.<sup>18</sup> However, the catalytic mechanism of nanoparticles, such as catalysis for the degradation of MO by Ag NPs, has not been deeply discussed yet.

In this work, the reduction of MO catalyzed by Ag NPs in the

presence of NaBH<sub>4</sub> has been studied. We tried to measure the different catalytic abilities of dispersed and aggregated Ag NPs. However, we are surprised to find that the dispersed Ag NPs could catalyze the degradation of MO, while the degradation products of MO could be catalyzed to form MO again during the aggregation of Ag NPs induced by CTAB. This suggested that there might be a reversible catalytic process for the degradation of MO. The strategy was illustrated in Scheme 1. The dispersed Ag NPs effectively catalyzed the reduction of MO to N,N-dimethyl-1,4-phenylenediamine and sodium sulfanilate in the presence of NaBH<sub>4</sub>, which resulted in the color change of the solution from orange to colorless. Interestingly, the addition of cetrimonium bromide (CTAB) into the solution to aggregate the Ag NPs<sup>12</sup> caused a distinct color change of solution back to orange. This indicated that N,N-dimethyl-1,4-phenylenediamine and sodium sulfanilate were catalyzed to form MO again. This discovery could contribute to the deep comprehension of the catalytic mechanism of nanoparticles in future.



Scheme 1. The reversible catalysis for the degradation of MO by citrate-capped Ag NPs in the presence of CTAB.

The citrate-capped Ag NPs<sup>19</sup> were prepared by reduction of AgNO<sub>3</sub> with NaBH<sub>4</sub> and sodium citrate (see ESI †).<sup>12</sup> The synthesized Ag NPs were well-dispersed and their diameters

were ca. 10 nm (Figure S1). The aggregated Ag NPs were prepared by adding CTAB into the citrate-capped Ag NPs solution. The dispersed and the aggregated Ag NPs were used to catalyze the degradation of MO in the presence of NaBH<sub>4</sub>. As shown in Figure 1A, after the addition of dispersed Ag NPs into the MO solution, the color of solution changed from orange to colorless rapidly (about 40s). When aggregated Ag NPs were added, the color of MO solution kept orange for 5 min and then gradually changed to colorless in 5 min. Figure S2 showed the time-dependent UV absorption at 250nm (A<sub>250</sub>) of the solution after adding aggregated Ag NPs. The absorption peak at 250 nm represents the reduction products of MO. The increase of A<sub>250</sub> suggested that MO was degraded. The results indicated that the catalytic activity of dispersed Ag NPs was much better than that of the aggregated Ag NPs.

Interestingly, with addition of CTAB into the degraded MO solution catalyzed by dispersed Ag NPs, the color of solution changed back to orange (Figure 1A). This indicated the regeneration of MO. The UV spectra of these solutions were recorded and shown in Figure 1B. In curve a, the absorbance band in the range of 400-550 nm represents the characteristic absorbance of MO. When Ag NPs were added to the MO solution, the characteristic absorbance of MO disappeared and the absorption peak at 250 nm emerged (curve b). In curve c, the absorbance band in the range of 400-550 nm reappeared and the absorption peak at 250 nm decreased in comparison to curve b. This indicated the oxidation of the reduction products to form MO. The experimental details see ESI†.

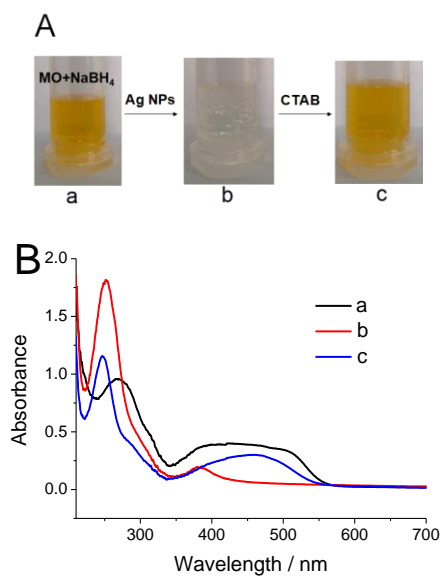


Figure 1. (A) Images of the MO solution containing NaBH<sub>4</sub> (a), solution a with the addition of Ag NPs (b) and the solution b with the addition of CTAB (c); (B) The corresponding UV spectra of the above solutions.

Reversible catalysis for the reaction between MO and NaBH<sub>4</sub> by Ag NPs was also confirmed by LC-MS. In Figure S3, the peak at t<sub>R</sub>=5.55 min corresponded to the MS peak at m/z 306.0 [M-Na+2H], which represents MO. As shown in Figure S4, the peak at t<sub>R</sub>=5.55 min disappeared, which indicated the successful

degradation of MO. The peak at t<sub>R</sub>=3.00 min corresponded to the MS peaks at m/z 218.0 [M+Na], 413.0 [2M+Na], 607.8 [3M+Na] and 802.7 [4M+Na]. These MS peaks were equally spaced with m/z 195. That means the substance was polymerized and its molecular weight should be 195.0. So it presents sodium sulfanilate, one of the reduction products of MO. The peak at t<sub>R</sub>=7.25 min corresponded to MS peaks at m/z 136.1 [M], which is consistent of the molecular weight of N,N-Dimethyl-1,4-phenylenediamine, the other reduction product of MO. To verify the above conclusion, the reduction products of MO catalyzed by Ag NPs were separated and purified. The NMR results confirmed that the reduction products of MO were sodium sulfanilate and N,N-Dimethyl-1,4-phenylenediamine (see ESI†). In Figure S5, the peak at t<sub>R</sub>=5.55 min recovered and the peaks at t<sub>R</sub>=3.00 min and t<sub>R</sub>=7.25 min decreased, which verified that the reduction products of MO reacted to form MO under the catalysis of Ag NPs.

The mechanism of the reversible catalysis for the reaction between methyl orange and NaBH<sub>4</sub> by silver nanoparticles is as follows. When MO molecules adsorbed onto the surface of dispersed Ag NPs, they were polarized and activated. The electron transfer between MO and NaBH<sub>4</sub> was accelerated and then the activation energy of reaction was reduced.<sup>6</sup> The products of the reaction between MO and NaBH<sub>4</sub> generated on the surface of Ag NPs and then diffused into solution. If the diffusion of these products was restricted, these products could be catalyzed to generate MO again. Thus, the reversible catalysis for the reaction between MO and NaBH<sub>4</sub> by Ag NPs could be observed.<sup>20</sup> When CTAB was added into the solution, the dispersed Ag NPs aggregated rapidly due to the hydrophobic effect. As shown in Figure 2, Ag NPs were agglomerate upon the addition of CTAB. In the aggregation process of Ag NPs, the products of the reaction between MO and NaBH<sub>4</sub> were wrapped in the hydrophobic layer and their diffusion to solution was restricted. Then they could be catalyzed to generate MO by Ag NPs. The catalytic activity of aggregated Ag NPs for the degradation of MO lowered largely due to their much smaller specific surface area. Therefore, the regenerated MO was not decomposed immediately and then could be observed.

The reaction process of N,N-dimethyl-1,4 phenylene diamine and sodium sulfanilate to form MO was shown in Scheme S1. NaBO<sub>2</sub> was oxidized to NaBO<sub>3</sub> by oxygen. NaBO<sub>3</sub> was a strong oxidant and it can oxidize the aniline to azo-compound.<sup>21</sup> Therefore, sodium sulfanilate was first oxidized to 4-nitrosobenzenesulfonic acid sodium salt due to the strong electron receptor effect of the sulfonic acid group.<sup>22</sup> And then 4-nitrosobenzenesulfonic acid sodium salt reacted with N,N-dimethyl-1,4 phenylene diamine to generate MO by the catalysis of aggregated Ag NPs.<sup>23</sup>

In order to verify the proposed mechanism of the regeneration of MO, several experiments were carried out to testify the function of oxygen and to simulate this reaction. As shown in Figure S8, the color of the degraded MO solution changed to yellow after the addition of CTAB (Figure S8, a). However, when the degraded MO solution was saturated with N<sub>2</sub>, the color remained colorless after the addition of CTAB (Figure S8, b). Subsequently, the solution was saturated with O<sub>2</sub> again and then its color changed to light yellow (Figure S9, b). It suggested that

dissolved oxygen was involved in the regeneration of MO. The color of the solution (Figure S9, b) was much lighter compared to the solution (Figure S8, a). It could be ascribed to the diffusion of the reaction products of MO and NaBH<sub>4</sub> into the solution.

Furthermore, the simulation experiment of the regeneration of MO was carried out. As shown in Figure S10, sodium sulfanilate and N,N-dimethyl-1,4-phenylenediamine could react to form MO in the presence of NaBO<sub>2</sub>, O<sub>2</sub> and aggregated Ag NPs induced by CTAB (curve b). In contrast, MO could not be generated if NaBO<sub>2</sub> was removed from the above solution (curve a). All the results proved that NaBO<sub>2</sub> and O<sub>2</sub> played important roles in the regeneration of MO, which was consistent with our assumption.

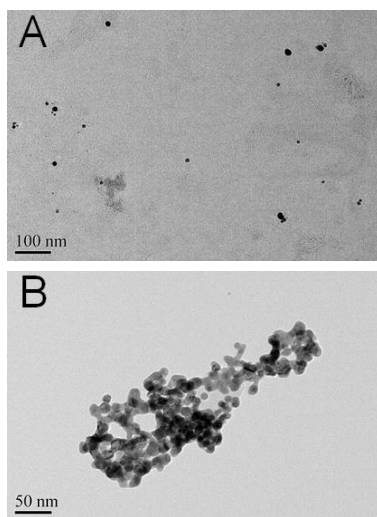


Figure 2. TEM images of the MO solution containing NaBH<sub>4</sub> and Ag NPs before (A) and after (B) the addition of 5 μM CTAB.

Furthermore, the reversible catalysis for the reaction between MO and NaBH<sub>4</sub> by Ag NPs was proved with the degradation of high concentration MO (1mM) catalyzed by Ag NPs. As shown in Figure 3, the color of the MO solution containing NaBH<sub>4</sub> with addition of Ag NPs changed from orange to near colorless, then changed back to light orange, finally changed to colorless. This indicated that MO degraded first, then regenerated partially, finally degraded completely. That means the reaction between MO and NaBH<sub>4</sub> catalyzed by Ag NPs is reversible for some extent. In contrast, the reversible degradation of MO in the concentration of 0.25 mM was not observed. It could be ascribed to the increased concentration of MO resulted in the higher concentration of degraded products around Ag NPs. Thus, more MO molecules were gradually regenerated by the catalysis of Ag NPs and then it could be observed by naked eyes. However, if the products of reaction between MO and NaBH<sub>4</sub> had already diffused into the solution, the regeneration of MO could not be observed. As shown in Figure 4, after Ag NPs had catalyzed the reaction between MO and NaBH<sub>4</sub> for 30 min, the addition of CTAB could not induce the regeneration of MO. It could be attributed to the low concentration of degraded products around Ag NPs.

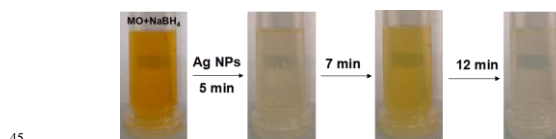


Figure 3. Images of the solution of MO containing NaBH<sub>4</sub> with the addition of Ag NPs taken at different time. Conditions: 300 μL of 1 mM MO solution mixed with 600 μL of 80 mM NaBH<sub>4</sub> solution, and then 400 μL Ag NPs was added to the solution.

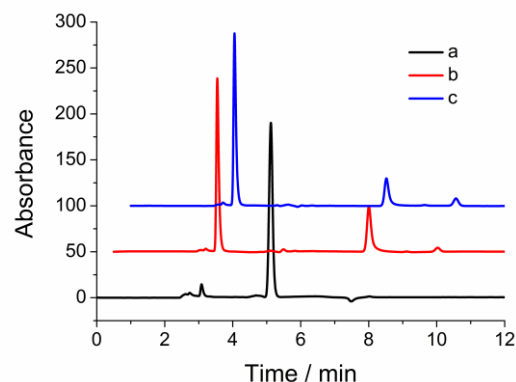


Figure 4. HPLC chromatograms of the MO solution containing NaBH<sub>4</sub> (a), solution a with addition of Ag NPs (b), solution b stood for 30 min and then was added 5 μM CTAB (c).

Anion surfactants could not induce the aggregation of citrate-capped Ag NPs.<sup>12</sup> Therefore, in according to the mechanism of the reversible catalysis by Ag NPs, the addition of SDS could not induce the regeneration of MO, which was identified with the experimental results shown in Figure 5.

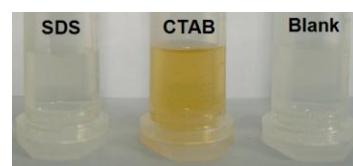


Figure 5. Images of the MO solution containing NaBH<sub>4</sub> and Ag NPs (Blank) upon the addition of 5 μM various surfactants.

The effect of the concentration of CTAB on the reversible catalysis by Ag NPs was studied. As shown in Figure 6, the color of the MO solution containing NaBH<sub>4</sub> and Ag NPs changed from colorless to orange gradually with the increase of the concentration of CTAB. The absorbance of the solution at 250 nm ( $A_{250}$ ) showed good linear relationship with the log[concentration of CTAB] in the range of 0.1-10 μM. The linear regression equation for CTAB was  $Y = -0.42208 - 0.30114X$ ,  $R = 0.9988$ , where Y is  $A_{250}$  and X is log[concentration of CTAB]. The LOD of CTAB is 0.5 μM. Thus, the interesting reversible catalysis by Ag NPs could be applied to the rapid detection of CTAB.

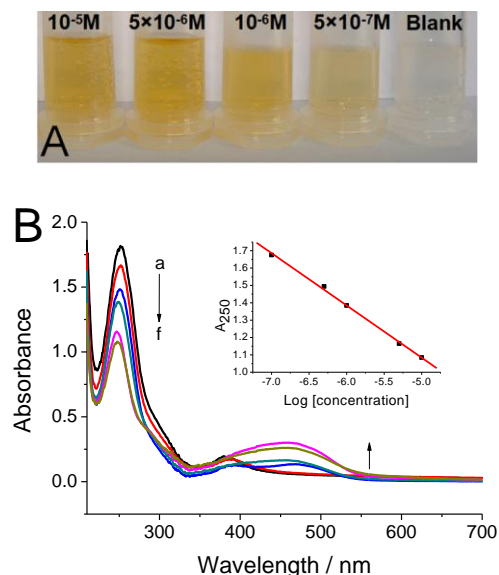


Figure 6. (A) Images of the MO solution containing NaBH<sub>4</sub> and Ag NPs (Blank) upon the addition of different concentration of CTAB; (B) UV spectra of the MO solution containing NaBH<sub>4</sub> and Ag NPs upon the addition of different concentration of CTAB. a-f corresponded to the addition of 0, 10<sup>-7</sup> M, 5 × 10<sup>-7</sup> M, 10<sup>-6</sup> M, 5 × 10<sup>-6</sup> M and 10<sup>-5</sup> M CTAB, respectively. Inset: plot of A<sub>250</sub> against log[CTAB].

In conclusion, the reversible catalysis for the reaction between MO and NaBH<sub>4</sub> by Ag NPs was first discovered. Substrate molecules were polarized and activated when they adsorbed onto the surface of Ag NPs. Thus the degradation of MO was largely enhanced by Ag NPs. When CTAB was added into the solution, the dispersed Ag NPs aggregated rapidly and the products of the reaction between MO and NaBH<sub>4</sub> were wrapped in the hydrophobic layer. Therefore, MO was regenerated by the catalysis of Ag NPs. The discovery of the reversible catalysis by nanoparticles may play an important role in studying the mechanism of nanocatalysis.

This work was supported by the National Instrumentation Program of China (2011YQ17006711), the Major Program of NSFC (21190044), the NSFC Scientific Equipment Joint Fund Project (11179004) and NSFC Innovative Research Group Project (21121091).

## Notes and references

State Key Laboratory of Analytical Chemistry for Life Science, School of Chemistry and Chemical Engineering, Nanjing University, Nanjing, 210093, P. R. China. Fax: +862583592774; Tel: +862583592774; E-mail: yuxd@nju.edu.cn;

† Electronic Supplementary Information (ESI) available: Experimental details, TEM image, time-dependent UV absorption graph and LC-MS results. See DOI: 10.1039/b000000x/

- (a) Fuan Wang, Xiaoqing Liu, Chun-Hua Lu and Itamar Willner, *ACS Nano*, 2013, 7, 7278; (b) Krishnendu Saha, Sarit S. Agasti, Chaekyu Kim, Xiaoning Li and Vincent M. Rotello, *Chem. Rev.*, 2012, 112, 2739.
- (a) Clemens Burda, Xiaobo Chen, Radha Narayanan and Mostafa A. El-Sayed, *Chem. Rev.* 2005, 105, 1025; (b) Susie Eustis and Mostafa A. El-Sayed, *Chem. Soc. Rev.* 2006, 35, 209; (c) Yujun Song, Weili Wei and Xiaogang Qu, *Adv. Mater.*, 2011, 23, 4215;

- (d) Juan Li, Hua-E. Fu, Ling-Jie Wu, Ai-Xian Zheng, Guo-Nan Chen and Huang-Hao Yang, *Anal. Chem.*, 2012, 84, 5309.
- (a) Hao Jing, Qingfeng Zhang, Nicolas Large, Chunmei Yu, Douglas A Blom, Peter Nordlander and Hui Wang. *Nano letters*, 2014, 14, 3674; (b) Emil Roduner, *Chem. Soc. Rev.*, 2006, 35, 583; (c) Didier Astruc, Feng Lu and Jaime Ruiz Aranzaes, *Angew. Chem., Int. Ed.*, 2005, 44, 7852; (d) Yongxing Hu, Yuzi Liu, Zheng Li and Yugang Sun, *Adv. Funct. Mater.*, 2014, 24, 2828; (e) Temer S. Ahmadi, Zhong L.Wang, Travis C.Green, Arnim Henglein and A. El-Sayed, *Science*. 1996, 272, 1924.
- (a) Jinrui Hao, Bin Xiong, XiaoDong Cheng, Yan He, and Edward S. Yeung. *Anal. Chem.*, 2014, 86, 4663; (b) Shenguang Ge, Fang Liu, Weiyang Liu, Mei Yan, Xianrang Song and Jinghua Yu, *Chem. Commun.*, 2014, 50, 475; (c) Sunghyun Kim, Jeong Won Park, Dongkyu Kim, Daejin Kim, In-Hyun Lee and Sangyong Jon, *Angew. Chem. Int. Ed.*, 2009, 48, 4138; (d) Yuexia Gao, Xing Li, Yonglong Li, Tianhua Li, Yayun Zhao and Aiguo Wu, *Chem. Commun.*, 2014, 50, 6447.
- (a) Sen Zhang, Shaojun Guo, Huiyuan Zhu, Dong Su and Shouheng Sun, *J. Am. Chem. Soc.*, 2012, 134, 5060; (b) Schrinner M, Ballauff M, Talmon Y, Kauffmann Y, Thun J, Müller M, Breu J., *Science*, 2009, 323, 617; (c) Nikesh Gupta, Henam Premananda Singh, Rakesh Kumar Sharma, *Colloids Surf. A*, 2010, 367, 102; (d) Qunyan Wei, Bin Li, Chao Li, Jiaqiang Wang, Wei Wang and Xiangjun Yang, *J. Mater. Chem.*, 2006, 16, 3606; (e) Arnim Henglein, *Langmuir*. 2001, 17, 2329.
- Nikesh Gupta, Henam Premananda Singh and Rakesh Kumar Sharma. *Journal of Molecular Catalysis A: Chemical*, 2011, 335, 248.
- (a) Ying Xue, Hong Zhao, Zhijiao Wu, Xiangjun Li, Yujian He and Zhuobin Yuan, *Analyst*, 2011, 136, 3725; (b) Sunghyun Kim, Jeong Won Park, Dongkyu Kim, Daejin Kim, In-Hyun Lee and Sangyong Jon, *Angew. Chem. Int. Ed.*, 2009, 48, 4138.
- Edit Csapó Rita Patakfalvi, Viktória Hornok, László Tamás Tóth, Áron Sipos, Anikó Szalai, Mária Cséte and Imre Dékány. *Colloids and Surfaces B: Biointerfaces*, 2012, 98, 43.
- (a) Guangke He, Liang Zhao, Kai Chen, Yuanyuan Liu and Hongjun Zhu, *Talanta*, 2013, 106, 73; (b) Eugenii Katz and Itamar Willner. *Angew. Chem. Int. Ed.*, 2004, 43, 6042.
- Nathaniel L. Rosi and Chad A. Mirkin, *Chem. Rev.*, 2005, 105, 1547.
- James E. Ghadiali and Molly M. Stevens, *Adv. Mater.*, 2008, 20, 4359.
- Li-Qing Zheng, Xiao-Dong Yu, Jing-Juan Xu and Hong-Yuan Chen, *Talanta*, 2014, 118, 90.
- Anand A. Kulkarni and Bhalchandra M. Bhanage, *ACS Sustainable Chem. Eng.*, 2014, 2, 1007.
- (a) A.-R. Vilchis-Nestor, J. Trujillo-Reyes, J. A. Colín-Molina, V. Sánchez-Mendieta and M. Avalos-Borja. *Int. J. Environ. Sci. Technol.*, 2014, 11, 977; (b) Nikesh Gupta, Henam Premananda Singh and Rakesh Kumar Sharma. *Colloids and Surfaces A: Physicochem. Eng. Aspects*. 2010, 367, 102.
- (a) Yunqing Zhu, Lang Fan, Bo Yang, and Jianzhong Du. *ACS Nano*. 2014, 8, 5022; (b) Lunhong Ai and Jing Jiang, *Bioresource Technology*, 2013, 132, 374.
- (a) Weiwei He, Xiaochun Wu, Jianbo Liu, Xiaona Hu, Ke Zhang, Shuai Hou, Weiya Zhou and Sishen Xie. *Chem. Mater.*, 2010, 22, 2988; (b) Huan Jiang, Zhaohui Chen, Haiyan Cao and Yuming Huang. *Analyst*, 2012, 137, 5560.
- Qunyan Wei, Bin Li, Chao Li, Jiaqiang Wang, Wei Wang and Xiangjun Yang. *J. Mater. Chem.*, 2006, 16, 3606.
- Subrata Kundu, *Phys. Chem. Chem. Phys.*, 2013, 15, 14107.
- Arnim Henglein and Michael Giersig, *J. Phys. Chem. B*. 1999, 103, 9533.
- Tarasankar Pal, Tapan K. Sau and Nikhil R. Jana, *Langmuir*. 1997, 13, 1481.
- S. M. Mehta, M. V. Vakilwala. *J. Am. Chem. Soc.*, 1952, 74, 563.
- Alexander McKillop, Jonathan A. Tarbin. *Tetrahedron Lett.*, 1983, 24, 1505.
- V. Castellana, D' Angelo, A.Gazz. *Chim. Ital.*, 1906, 36, 56.